Journal of Alloys and Compounds 509 (2011) 9685–9691

Contents lists available at ScienceDirect

Journal of Alloys and Compounds

journal homepage: www.elsevier.com/locate/jallcom

Bismuth-containing semiconductors: Linear and nonlinear optical susceptibilities of $GaAs_{1-x}Bi_x$ alloys

Ali Hussain Reshak[a,b,*], H. Kamarudin[b], S. Auluck[c]

[a] Institute of Physical Biology, South Bohemia University, Nove Hrady 37333, Czech Republic
[b] School of Material Engineering, Malaysia University of Perlis, P.O. Box 77, d/a Pejabat Pos Besar, 01007 Kangar, Perlis, Malaysia
[c] National Physical Laboratory, Dr. K S Krishnan Marg, New Delhi 110012, India

ARTICLE INFO

Article history:
Received 24 June 2011
Received in revised form 25 July 2011
Accepted 28 July 2011
Available online 3 August 2011

Keywords:
$GaAs_{1-x}Bi_x$ alloys
Optical properties (linear and nonlinear)
DFT
FP-LAPW

ABSTRACT

Using all electron full potential – linearized augmented plane wave (FP-LAPW) method the linear and nonlinear optical susceptibilities of cubic $GaAs_{1-x}Bi_x$ alloys with x varying between 0.25 and 0.75 with increment of 0.25 are investigated. We have applied the generalized gradient approximation (GGA) for the exchange and correlation potential. In addition the Engel–Vosko generalized gradient approximation (EVGGA) was used. The reflectivity, refractivity, absorption coefficient and the loss function of these ternary alloys were investigated. The absorption coefficient shows that $GaAs_{0.25}Bi_{0.75}$ possess the highest coefficient among the investigated alloys which supports our previous observation that the band gap decreases substantially with increasing Bi content and the materials with very small energy band gap possess the highest absorption coefficient. The investigation of the linear and nonlinear optical susceptibilities of $GaAs_{1-x}Bi_x$ shows a strong band gap reduction as commonly found experimentally.

1. Introduction

III–V Bi doped ternary alloys such as $GaAs_{1-x}Bi_x$ have attracted a great deal of interest due to their significance in potential applications such as solar cells, optoelectronic, semiconductor lasers, and optical detectors [1]. Doping GaAs compound by a low concentration of Bi is found to have a significant influence on electronic structure and optical properties of these compounds. Madouri et al. [2] have observed a huge reduction in the band gap by replacing just 1% of the arsenic by Bi. Ever since this discovery, intensive efforts have been devoted to investigate the effect of increasing Bi concentration on the properties of such doped alloys. The main feature of each solar cell is its capability to absorb effectively wide spectrum of photons contained in solar radiation reaching its active surface. This feature depends on intrinsic optical and electronic properties of semiconductor material, and the critical parameter related to semiconductor is energy band gap and its dispersion in k-space. The photons with energy lower than the energy band gap cannot be absorbed. On the other hand one photon, even if its energy exceeds doubled value of that of the band gap, cannot generate more than single electron–hole pair, dissipating all its excess energy as a heat in the cell. The role of the absorber with these limitations in the conventional solar cell has been explained below. Another factor is the mobility of principal carriers, i.e. holes and electrons which are depend on the effective mass and in turn on the energy band dispersion in k-space.

For using wide band semiconductor, light absorption becomes limited only to high energy photons. The result is in lower photocurrent but the advantages are more efficient energy conversion of the absorbed high energy part of solar spectrum because higher fraction of photons energy is being converted into electricity, subsequently higher value of the output voltage is obtained. While solar cells made using narrow band gap semiconductors that are capable of absorbing larger spectral part of solar spectrum and exhibit higher photocurrent values but have lower energy conversion efficiency and produce lower output voltage. Alloys fabricated from elements of the groups III and V have proven to be optimal compounds for semiconductor devices. Almost every combination of this elements have been tried in order to obtain a semiconductor material with desired properties. However, thallium and bismuth, the biggest and heaviest elements in these groups, have been ignored due to their size and the tendency to surface segregate during their growth [3]. In order to incorporate the bismuth atom into the lattice it is necessary to reduce the competition for the group V sites and to overcome this segregation tendency. This can be achieved with low growth temperatures and nearly stoichiometric III:V flux ratios [4].

Due to the size of this element, compressive strain is achieved when incorporated to the crystal structural as a substitutional alloy, taking the place of an arsenic atom [5]. With this size increment,

* Corresponding author at: Institute of Physical Biology, South Bohemia University, Nove Hrady 37333, Czech Republic. Tel.: +420 777 729583; fax: +420 386 361255.
E-mail address: maalidph@yahoo.co.uk (A.H. Reshak).

0925-8388/$ – see front matter © 2011 Elsevier B.V. All rights reserved.
doi:10.1016/j.jallcom.2011.07.086

the band structure modifies provoking a strong band reduction. The reduction of the band gap is also expected since an addition of a metal material is being added to the GaAs semiconductor compound. In 2006 Young [6] reported that; the use of Bi as a surfactant progressed [7] to successful recent attempts to incorporate Bi into GaAs. This was achieved by significant deviation from typical GaAs growth conditions in molecular beam epitaxy (MBE) [8]. GaAsBi, is nonconventional alloys, in the sense that the alloying element (Bi) introduces bound states in addition to energy bands, and behaves more like an isoelectronic donor (Bi) than a true alloying element [6,1]. The large reduction in band gap due to Bi is thought to be due to a resonant interaction is expected between the Bi 6p state and the valence band maximum [6,1].

The growing demand for new technologies coupled with the unusual properties of these materials provides the motivation for the current study. In this paper linear and nonlinear optical susceptibilities study based on density functional theory (DFT) of the $GaAs_{1-x}Bi_x$ ternary alloy is performed with and without spin orbit coupling (SOC). By varying the composition of bismuth, a comparison of the effect of additional Bi is analyzed.

In Section 1, we present brief idea of what have been done. The rest is organized as follows: Section 2 is devoted for the method of calculation. The results and discussion are presented in Section 3, and Section 4 summarizes the main concluding points.

2. Method of calculation

The calculations of the linear and nonlinear optical susceptibilities were carried out using the full potential linearized augmented plane wave (FP-LAPW) method as implemented in WIEN2K code [9]. The exchange correlation potential was treated using the generalized gradient approximation (GGA) [10] for the total energy calculations. Additionally we have used the Engel–Vosko generalized gradient approximation (EV-GGA) [11], which optimizes the corresponding potential for electronic band structure calculations. It is well known in the self-consistent band structure calculation within DFT method (both of LDA and GGA approaches) usually underestimate the energy gap [12]. This is mainly due to the fact that they are based on simple model assumptions which are not sufficiently flexible to accurately reproduce the exchange correlation energy and its charge space derivative. Engel and Vosko considered this shortcoming and constructed a new functional form of GGA [11] which is able to reproduce better exchange potential at the expense of less agreement in the exchange energy. This approach (EV-GGA) yields better band splitting than the GGA. The total energy calculations are performed for $GaAs_{1-x}Bi_x$ (x = 0.25, 0.5 and 0.75). In this work, we have used the 'special quasi-random structures' (SQS) approach of Zunger et al. [13] to reproduce the randomness of the alloys for the first few shells around a given site. This approach is reasonably sufficient to describe the alloys for many physical properties that are not affected by the errors introduced by using the concept of periodicity beyond the first few shells.

The spherical harmonics inside non-overlapping muffin-tin (MT) spheres surrounding the atomic are expanded up to l_{max} = 10. The muffin-tin radii are 1.6 atomic units (a.u.) for Bi, whereas a 1.95 a.u. is used for both Ga, and As. The plane wave cut-off of K_{max} = 7.0/RMT was chosen for the expansion of the wavefunctions in the interstitial region for all the binary compounds $GaAs_{1-x}Bi_x$ ternary alloys. The charge density was Fourier expanded up to G_{max} = 14 (Ryd)$^{1/2}$.

We have optimized the atomic positions of $GaAs_{1-x}Bi_x$ ternary alloys (structural relaxation), by minimization of the forces (1 mRy/au) acting on the atoms. Using the relaxed geometry various spectroscopic features including the linear and nonlinear optical dispersions can be calculated. Once the forces are minimized in this construction one can then find the self-consistent density at these positions by turning off the relaxations and driving the system to self-consistency. The calculations were done with and without spin orbit coupling. We carefully examine the spin orbit coupling effect on Bi and As split-off band. In Fig. 1, we give prototype in low symmetry band structure of alloys near the Fermi energy to distinguish between Bi-6p heavy holes (HH), Bi-6p light hole (LH) and As/Bi spilt-off bands.

Self-consistency was achieved by use of 500 k-points in the irreducible Brillouin zone (IBZ). The linear and nonlinear optical susceptibilities are calculated using 1400 k-points in the IBZ. Both the muffin-tin radius and the number of k-points were varied to ensure total energy convergence. The self-consistent calculations are converged since the total energy of the system is stable within 10^{-5} Ry.

Table 1
The optimized atomic position, these ternary alloys are modeled using the SQS approach. We give the optimized positions of the Ga atoms by minimizing the forces on the atoms whereas the other atoms at symmetry positions where force is always zero.

Compound	X	Y	Z
$GaAs_{0.75}Bi_{0.25}$ (space group P-43m #215)			
Ga	0.22233381	0.77766619	0.77766619
	0.77766619	0.22233381	0.77766619
	0.77766619	0.77766619	0.22233381
	0.22233381	0.22233381	0.22233381
As	0.0	0.5	0.5
	0.5	0.0	0.5
	0.5	0.5	0.0
Bi	0.0	0.0	0.0
$GaAs_{0.5}Bi_{0.5}$ (space group P222 #16)			
Ga	0.25000016	0.25000004	0.19998184
	0.74999984	0.74999996	0.19998184
	0.25000016	0.74999996	0.80001816
	0.74999984	0.25000004	0.80001816
Bi	0.0	0.0	0.0
Bi	0.5	0.5	0.0
As	0.5	0.0	0.5
$GaAs_{0.25}Bi_{0.75}$ (space group P-43m #215)			
Ga	0.27229100	0.72770900	0.72770900
	0.72770900	0.27229100	0.72770900
	0.72770900	0.72770900	0.27229100
	0.27229100	0.27229100	0.27229100
Bi	0.0	0.5	0.5
	0.5	0.0	0.5
	0.5	0.5	0.0
As	0.0	0.0	0.5

3. Results and discussion

3.1. Structural properties

In this section, we present the structural properties of the $GaAs_{1-x}Bi_x$ compounds for compositions x = 0.25, 0.5 and 0.75. The binary alloys, GaBi and GaAs are described by zinc-blende structure, whereas the ternary alloys are modeled using the SQS approach [13]. For the composition x = 0.25 and 0.75 the simplest structure is an eight-atom simple cubic lattice (luzonite): the cations with the lower concentration form a regular simple cubic lattice. For x = 0.5, the smallest ordered structure is (0 0 1) supercell (see Table 1). In Table 1 we give the optimized positions of the Ga atoms by minimizing the forces on the atoms. The volumes of all the compounds were optimized by calculating the total energy as a function of volume, which was followed by fitting the results with Murnaghan's equation of state [14]. From this fitting, we obtained the optimum lattice constant and bulk modulus. Fig. 2 presents our calculated values obtained after optimization with and without SOC effect mainly on Bi site. From this figure one can notice that the optimized lattice constants agree well with those estimated by Vegard's law [15] for the case of binary systems. However, in the case of the ternary alloys, the lattice constants deviate from the estimated values using Vegard's law [15]:

$$a(AB_{1-x}C_x) = xa_{AC} + (1-x)a_{AB} \tag{3.1}$$

where a_{AC} and a_{AB} are the equilibrium lattice constants of the binary compounds AC and BC, respectively and $a(AB_{1-x}C_x)$ is the alloy lattice constant. The relation of the lattice constant exhibits a quadratic term as a result of the mismatch between the lattice constants of the extreme binary alloys, AB and AC. Therefore, the lattice constant is better described as follows:

$$a(AB_{1-x}C_x) = xa_{AC} + (1-x)a_{AB} - x(1-x)b \tag{3.2}$$

Here, the constant b is the bowing parameter. The bowing in lattice constants of $GaAs_{1-x}Bi_x$ compounds is −1.004 (without SOC)

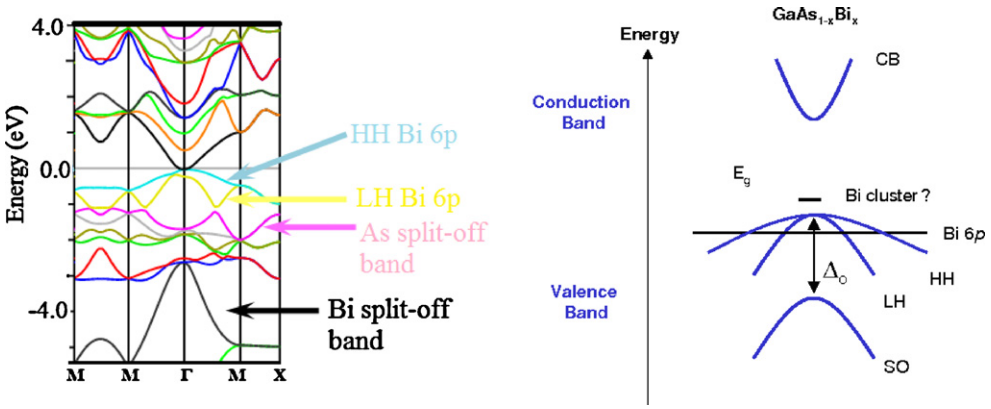

Fig. 1. Close prototype of band diagram for alloys to understand the spin orbit split-off band variation of As/Bi p band on applying SOC.

and −0.929 (with SOC), where negative sign indicates the increase in lattice constant from GaAs → GaBi presented in Fig. 2(a), using the GGA approximations. This observation agreed well with the experimental observation of Oe and Okamoto [16]. The variation of bulk modulus versus Bi content proves the decreasing change of $GaAs_{1-x}Bi_x$ alloy consistent (from GaAs → GaBi) with bowing parameter +60.46 (without SOC) and 54.72 (with SOC), see Fig. 2(b). In Fig. 2, we observe that at concentration up to 25% of Bi there is no obvious change is lattice parameter as well as on bulk modulus by adding SOC on Bi site, which is due to the low concentration of Bi. But at higher concentration of Bi the bowing is smaller due to addition of SOC effect in both lattice parameter and bulk modulus. Thus, high content of Bi at $GaAs_{1-x}Bi_x$ gives a recommendation for optoelectronic devices applications.

3.2. Linear optical susceptibilities

As it has mentioned above that both LDA and GGA lead to underestimate the energy band gaps in semiconductors and since the energy band differences enter the calculations of response functions in the denominators of the expressions they will play a major rule in the values of the susceptibilities, so it is not surprising that the latter values will be overestimated. That will lead to errors of the order of 10–30% in linear response. The problem is aggravated in higher-order responses by the fact that denominators occur in higher powers [17]. In order to overcome this shortcoming we have used the EV-GGA approach. The linear response of the system to electromagnetic radiation can be described by means of the dielectric function $\varepsilon(\omega)$ which is related to the interaction of photons with electrons. Two kinds of contributions to $\varepsilon(\omega)$ are usually distinguished, namely intra-band and inter-band electronic excitations. Intra-band transitions are not present in semiconductors, as they are present only for metals and semi-metals. The dispersion of the imaginary part of the dielectric function $\varepsilon_2(\omega)$ can be calculated from the momentum matrix elements between the occupied and unoccupied wavefunctions, giving rise to the selection rules. The real part $\varepsilon_1(\omega)$ of the dielectric function can be evaluated from the imaginary part $\varepsilon_2(\omega)$ by the Kramer–Kronig relationship [18]. All the other optical constants can be derived from $\varepsilon_1(\omega)$ and $\varepsilon_2(\omega)$. To calculate the optical spectra of the dielectric function, $\varepsilon(\omega)$, a dense mesh of uniformly distributed k-points is required. Hence, the Brillouin zone integration was performed with 1400 k-points in the irreducible part of the Brillouin zone for both linear and non-linear optical susceptibilities, with broadening equal to 0.1 eV to bring out all the structures. This value is typical of the experimental accuracy.

Fig. 3a, display the imaginary and real parts of the electronic dielectric function $\varepsilon(\omega)$ spectra for a spectral energies up to 14.0 eV for the cubic structure of $GaAs_{1-x}Bi_x$ (x = 0.25, 0.5, 0.75). The analysis of $\varepsilon_2(\omega)$ curve shows that all the compounds presented two main peaks situated at 2.5 and 5.0 eV. The origin of these peaks is attributed to the inter-band transitions form the occupied Ga-s/p/d and As/Bi-s/p/d band states to the unoccupied Ga-s/p and As/Bi-s/p/d band states. Following Fig. 3a one can see that the structures of $\varepsilon_2(\omega)$ for all the alloys are spectrally shifted towards lower energies with increasing the amplitude when the concentration of Bi increases, which confirms our previous observation that the energy band gap is reduced with increasing the concentration of Bi.

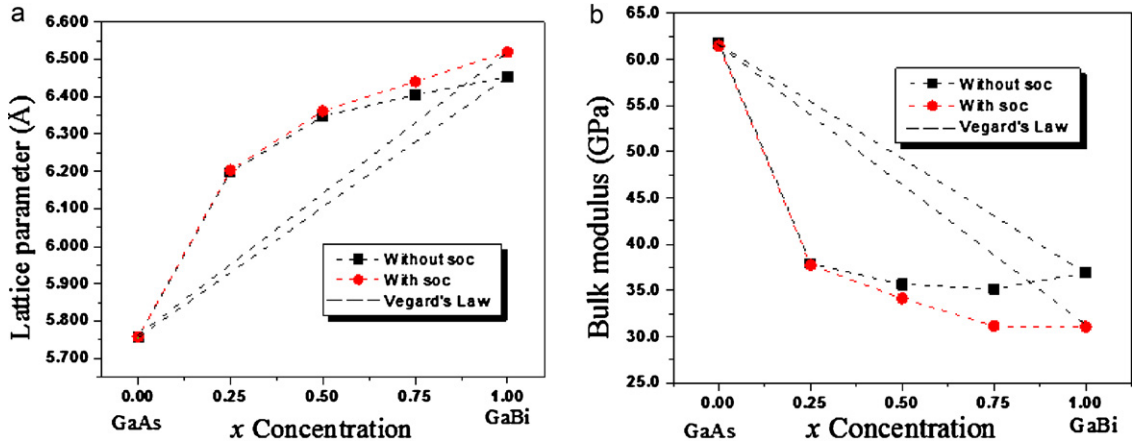

Fig. 2. Variation of calculated lattice parameter and bulk modulus with and without taking into account of spin orbit coupling versus Bi concentration in $GaAs_{1-x}Bi_x$ <!– no-mfc –>(also comparison with Vegard's law)<!– /no-mfc –>.

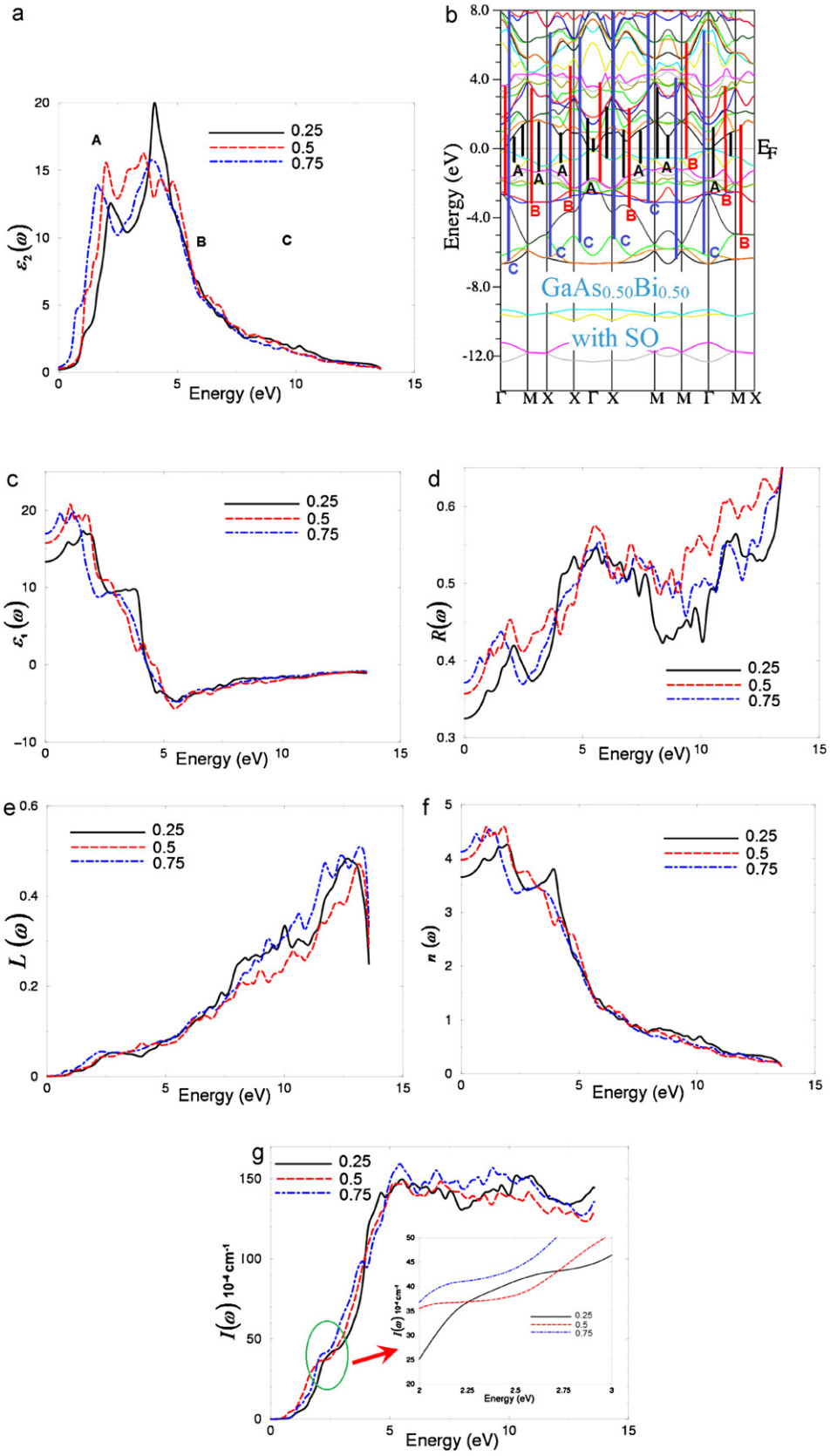

Fig. 3. (a) Calculated $\varepsilon_2(\omega)$ spectra. (b) The calculated band structure along with the optical transitions depicted on a generic band structure of the cubic $GaAs_{0.5}Bi_{0.5}$ as prototype. (c) Calculated $\varepsilon_1(\omega)$ spectra. (d) Calculated reflectivity $R(\omega)$. (e) Calculated loss function $L(\omega)$. (f) Calculated refractive index $n(\omega)$. (g) Calculated absorption coefficient $I(\omega)$. For the cubic $GaAs_{1-x}Bi_x$ (x = 0.25, 0.5, 0.75).

Table 2
Calculated static dielectric constants $\varepsilon_1(0)$, $n(0)$, $\left|\chi^{(2)}_{123}(0)\right|$ (pm/V), $\left|\chi^{(2)}_{123}(\omega)\right|$ (pm/V) at 1064 nm.

Components	$\chi^{(2)}_{123}(0)$ (pm/V)	$\chi^{(2)}_{123}(\omega)$ at λ = 1064 nm (pm/V)	$\varepsilon_1(0)$	$n(0)$
$GaAs_{0.75}Bi_{0.25}$	9.0	16	13.5	3.7
$GaAs_{0.5}Bi_{0.5}$	10.0	16.5	16.0	4.0
$GaAs_{0.25}Bi_{0.75}$	11.5	18.5	17.0	4.2

In order to identify the spectral peaks in the linear optical spectra we considered the optical transition matrix elements. We used our calculated band structure to indicate the transitions, indicating the major structure for the principal components $\varepsilon_2(\omega)$ in the band structure diagram. These transitions are labeled according to the spectral peak positions in Fig. 3a. For simplicity we have labeled the transitions in Fig. 3b, as *A*, *B*, and *C*. The transitions (*A*) are responsible for the structures for $\varepsilon_2(\omega)$ in the spectral range 0.0–5.0 eV; the transitions (*B*) 5.0–10.0 eV, and the transitions (*C*) 10.0–14.0 eV. As prototype we show these transitions only for $GaAs_{0.5}Bi_{0.5}$. The calculated $\varepsilon_1(\omega)$ are shown in Fig. 3c and the estimated values of the static optical dielectric constant $\varepsilon_1(0)$, which is also called higher frequency dielectric constant because it does not include the phonon effect, are listed in Table 2.

The calculations of the frequency-dependent dielectric function involve the energy eigenvalues and electron wave functions. These components $\varepsilon_2(\omega)$ are determined by inter-band transitions from valence- into conduction-band states. According to the dipolar selection rule only transitions changing the angular momentum quantum number l by unity ($\Delta = \pm 1$) are allowed. The electronic band structure of these alloys suggests that the first peak in $\varepsilon_2(\omega)$ is due to the transition from Ga-p, As-p, Bi-p states to Ga-s/p, As-p and Bi-s/p/d states, while the second peak corresponding to the Ga-s/p and Bi-p to Ga-p/d and Bi-s/p/d states. A remarkable fact regarding the first peak in $\varepsilon_2(\omega)$ is that its width is essentially determined by the width of the highest occupied valence band.

The calculated optical reflectivity spectra as shown in Fig. 3d, are started at about 0.02% and have a maximum value of roughly 25% at energy about 6.0 eV. The reflectivity spectrum reproduces the positions of the peaks determined by inter-band transitions with a good accuracy. It is interesting that there is an abrupt reduction in the reflectivity spectrum between 9.0 and 11.0 eV confirming the occurrence of a collective plasmon resonance. The depth of the plasmon minimum is determined by the imaginary part of the dielectric function at the plasma resonance and is representative of the degree of overlap between the inter-band absorption regions.

In Fig. 3e, the energy loss function is plotted in basal-plane and in direction of *c*-axis. The plasmon losses correspond to collective excitations of the valence electrons and their energies are related to the density of valence electrons. In the case of inter-band transitions, which consist mostly of plasmon excitations, the scattering probability for volume losses is directly connected to the energy loss function. There are other features in this spectrum, in addition to the plasmon peak, associated with inter-band transitions. The plasmon spectral peak is usually the most intense feature in the spectrum and this is at energy where $\varepsilon_1(\omega)$ goes to zero. The energy of the maximum peak of $(-\varepsilon_1(\omega))^{-1}$ at ~12.5 eV for these alloys which are assigned to the energy of volume plasmon $\hbar\omega_p$.

The calculated refractive index dispersions $n(\omega)$ are shown in Fig. 3f. The calculated values of $n(\omega)$ at static limit and at λ = 1064 nm are listed in Table 2. Following Fig. 3f one can emphasize that at around 4.0 eV these alloys possesses high refractive indices decreasing at higher energies.

Fig. 3g shows the absorption coefficient of these alloys is zero below the fundamental energy band gap, then increases rapidly to form the first absorption peak at around 5.0 eV. Then the absorption coefficient started to oscillate around the value of 150×10^{-4} cm^{-1} to show the stability in the absorption coefficient at higher energies. Fig. 3g shows that $GaAs_{0.25}Bi_{0.75}$ have the highest absorption coefficient among the other compounds that is attributed to the fact that $GaAs_{0.25}Bi_{0.75}$ possess the smallest energy band gap which support our previous observation that $GaAs_{0.25}Bi_{0.75}$ is the best compound for solar cells.

3.3. Nonlinear optical susceptibilities (second harmonic generation)

Since $GaAs_{1-x}Bi_x$ alloys have cubic structure the symmetry allows only one nonzero component namely; $\chi^{(2)}_{123}(-2\omega;\omega;\omega)$. The complex second-order nonlinear optical susceptibility tensor $\chi^{(2)}_{123}(-2\omega;\omega;\omega)$ has been calculated using the expressions given in Refs. [19–21]. The formalisms for calculating the second order susceptibility $\chi^{(2)}_{123}(-2\omega;\omega;\omega)$ for non-magnetic semiconductors and insulators based on the FP-LAPW method have been presented before [20,21]. In the first order responses (linear responses) functions, only the inter-band terms appear and involve only the square of matrix elements, which ensures, for example that $\varepsilon_2(\omega)$ is positive. The second harmonic response involves 2ω resonance in addition to the ω resonance. Both ω and 2ω resonances can be additionally divided into inter-band $\chi^{(2)}_{123}(-2\omega;\omega;\omega)$, intra-band $\chi^{(2)}_{123}(-2\omega;\omega;\omega)$ contributions and the modulation on inter-band terms by intra-band terms $\chi^{(2)}_{123}(-2\omega;\omega;\omega)$ [19–22]. The dipole matrix element values are much stronger in nonlinear case. The real and imaginary parts of the products of matrix elements that determine the strength of a given resonance in $\chi^{(2)}_{123}(-2\omega;\omega;\omega)$ can be positive or negative. The imaginary part of the $\chi^{(2)}_{123}(-2\omega;\omega;\omega)$ for ternary $GaAs_{0.75}Bi_{0.25}$, $GaAs_{0.5}Bi_{0.5}$, $GaAs_{0.25}Bi_{0.75}$, alloys is shown in Fig. 4a. We should emphasize that increasing the concentration of Bi leads to increase the amplitude and shift all the structures of $\chi^{(2)}_{123}(-2\omega;\omega;\omega)$ towards lower energies that is indicated that increasing the concentration of Bi leads to increase the value of the second harmonic generation.

The nonlinear optical dispersions are much more sensitive to small changes in the band structure dispersions and more complicated than the linear ones. The difficulties concern both the numerical and the physics because more conduction bands and more *k*-points are required to reach a reasonable accuracy. We should emphasize that calculating the complex second-order nonlinear optical susceptibility tensors with LDA results in incorrect complex second-order nonlinear optical susceptibility tensors since they are more sensitive to the band gap than the linear one due to higher power energy differences in the denominators of the formalism of the complex second-order nonlinear optical susceptibility tensors [20,23]. To avoid the problem of the well-known LDA underestimation of the band gap we have used EV-GGA. We have found that EV-GGA have significant influence on the second-order nonlinear optical dispersion since it reproduces better band gap with respect to experiment, however it is still underestimate energy band gap by around 10%. To avoid this drawback we consider quasiparticle self-energy corrections at the level of scissors operators in which the energy bands are rigidly shifted to merely bring the calculated energy gap close to the experimental gap, see Fig. 3a.

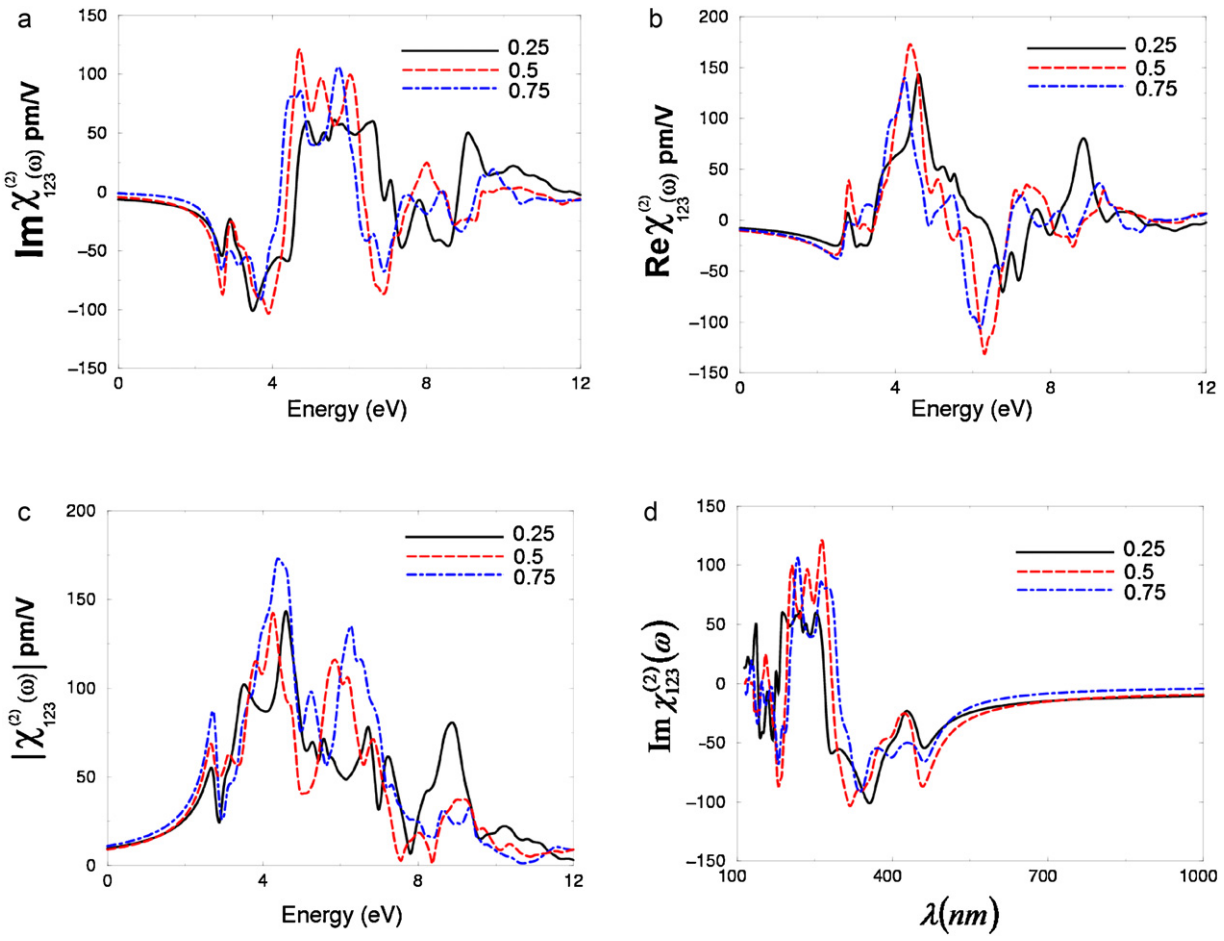

Fig. 4. (a) Calculated *Im* $\chi^{(2)}_{123}(\omega)$ spectra. (b) Calculated *Re* $\chi^{(2)}_{123}(\omega)$. (c) Calculated $\left|\chi^{(2)}_{123}(\omega)\right|$. (d) Calculated nonlinear spectroscopy. For the cubic $GaAs_{1-x}Bi_x$ (x = 0.25, 0.5, 0.75).

Looking at Fig. 4b one can see that the values of Re $\chi^{(2)}_{123}(0)$ decreases from −7.5 pm/V ($GaAs_{0.75}Bi_{0.25}$), −9.5 pm/V ($GaAs_{0.5}Bi_{0.5}$), −10.5 pm/V ($GaAs_{0.25}Bi_{0.75}$). That is attributed to the fact that the nonlinear optical properties are more sensitive to small changes in the band structure than the linear optical properties because the second harmonic response involves 2ω resonance terms in addition to the usual ω resonance and the threshold for 2ω parts occurs at the half energy of the threshold for ω part, as a result, only the 2ω inter/intra terms contributes to $\chi^{(2)}_{123}(-2\omega;\omega;\omega)$ in the energy range below the fundamental energy band gap. The complex second-order nonlinear optical susceptibility tensors $\chi^{(2)}_{ijk}(\omega)$ are formed both by the 2ω resonance in addition to the usual ω resonance. Both ω and 2ω resonances can be further separated into inter-band and intra-band contributions. Fig. 4c displays our calculated $\left|\chi^{(2)}_{123}(-2\omega;\omega;\omega)\right|$. Again it shows that with increasing Bi content all the spectral structures of $\left|\chi^{(2)}_{123}(-2\omega;\omega;\omega)\right|$ are shifted towards lower energies with increasing the values of $\left|\chi^{(2)}_{123}(0)\right|$ as a function of the Bi concentration. These values and $\left|\chi^{(2)}_{123}(-2\omega;\omega;\omega)\right|$ at λ = 1064 nm are given in Table 1. Therefore, the static values of the second order susceptibility tensor are very important and can be used to estimate their relative second harmonic generation (SHG) efficiency. From Fig. 4d, showing the nonlinear spectroscopy of these alloys, it is clear that these alloys show considerable nonlinear optical spectra in the wavelength starting from vacuum ultraviolet spectral range up to infrared that's make these alloys to be applicable in this wide spectral range.

4. Conclusions

This article is devoted to very important topic of modern aspects of theoretical and experimental physical chemistry to study the dispersion of linear and nonlinear optical susceptibilities in important materials. In the present work the calculation of the linear and nonlinear optical susceptibility dispersions for $GaAs_{0.75}Bi_{0.25}$, $GaAs_{0.5}Bi_{0.5}$ and $GaAs_{0.25}Bi_{0.75}$ alloys were performed. We have calculated the complex second-order optical susceptibility dispersions for the principal tensor component $\chi^{(2)}_{123}(\omega)$ and its zero-frequency limit. In the theoretical calculations we have used the relaxed geometry after optimization the crystalline structure of $GaAs_{0.75}Bi_{0.25}$, $GaAs_{0.5}Bi_{0.5}$ and $GaAs_{0.25}Bi_{0.75}$ alloys. The state-of-the-art full potential linear augmented plane wave method, based on the density functional theory was applied.

Acknowledgements

This work was supported from the institutional research concept of the Institute of Physical Biology, UFB (No. MSM6007665808), the program RDI of the Czech Republic, the Project CENAKVA (No. CZ.1.05/2.1.00/01.0024), the Grant No. 152/2010/Z of the Grant Agency of the University of South Bohemia. School of Material Engineering, Malaysia University of

Perlis, P.O. Box 77, d/a Pejabat Pos Besar, 01007 Kangar, Perlis, Malaysia.

References

[1] Y. Zhang, A. Mascarenhas, L.-W. Wang, Phys. Rev. B 71 (2005) 155201.
[2] D. Madouri, A. Boukra, A. Zaoui, M. Ferhat, Comput. Mater. Sci. 43 (2008) 818.
[3] M.J. Antonell, C.R. Abernathy, A. Sher, M. Berding, M. Van Schilfgaarde, A. Sanjuro, K. Wong, J. Cryst. Growth 188 (1998) 113.
[4] R.B. Lewis, D.A. Beaton, X. Lu, T. Tiedje, J. Cryst. Growth 311 (2009) 1872–1875.
[5] K. Takahiro, K. Kawatsura, K. Oe, F. Nishiyama, J. Electron. Mater. 32 (1) (2003) 34–37.
[6] E.C. Young, GaNAs and GaAsBi: structural and electronic properties of two resonant state semiconductor alloys, PhD thesis, University of British Columbia, 2006.
[7] S. Tixier, M. Adamcyk, E.C. Young, J.H. Schmid, T. Tiedje, J. Cryst. Growth 251 (2002) 449–454.
[8] S. Tixier, M. Adamcyk, T. Tiedje, S. Francoeur, A. Mascarenhas, P. Wei, F. Schiettekatte, Appl. Phys. Lett. 82 (14) (2003) 2245–2247.
[9] P. Blaha, K. Schwarz, G.K.H. Madsen, D. Kvasnicka, J. Luitz, 2001 WIEN2K, Techn. Universitat, Wien, Austria, ISBN 3-9501031-1-1-2.
[10] J.P. Perdew, S. Burke, M. Ernzerhof, Phys. Rev. Lett. 77 (1996) 3865.
[11] E. Engel, S.H. Vosko, Phys. Rev. B 47 (1993) 13164.
[12] P. Dufek, P. Blaha, K. Schwarz, Phys. Rev. B 50 (1994) 7279.
[13] A. Zunger, S.-H. Wei, L.G. Feireira, J.E. Bernard, Phys. Rev. Lett. 65 (1990) 353.
[14] F.D. Murnaghan, Proc. Natl. Acad. Sci. U. S. A. 30 (1944) 244.
[15] L. Vegard, Z. Phys. 5 (1921) 17.
[16] K. Oe, H. Okamoto, Jpn. J. Appl. Phys. 37 (11A) (1998) L1283–L1285.
[17] S.N. Rashkeev, W.R.L. Lambrecht, B. Segall, Phys. Rev. B 57 (1998) 9705.
[18] H.Z. Tributsch, Naturforsch. A 32A (1977) 972.
[19] D.R. Penn, Phys. Rev. 128 (1962) 2093.
[20] A.H. Reshak, PhD thesis, Indian Institute of Technology – Roorkee, India, 2005.
[21] S. Sharma, C. Ambrosch-Draxl, Phys. Scripta T 109 (2004) 128.
[22] S. Sharma, J.K. Dewhurst, C. Ambrosch-Draxl, Phys. Rev. B 67 (2003) 165332.
[23] S.N. Rashkeev, W.R.L. Lambrecht, Phys. Rev. B 63 (2001) 165212;
S.N. Rashkeev, W.R.L. Lambrecht, B. Segall, Phys. Rev. B 57 (1998) 3905–3919.